

To appear in the Astronomical Journal

Variable Stars in the Fornax Dwarf Galaxy

D. Bersier

Harvard-Smithsonian Center for Astrophysics, 60 Garden St, Cambridge MA 02138

P. R. Wood

Research School of Astronomy & Astrophysics, Australian National University, Mount Stromlo Observatory, Private Bag, Weston Creek PO, ACT 2611, Australia

ABSTRACT

We present a search for variable stars in the Fornax dwarf galaxy covering an area of 1/2 a square degree. We have ~ 30 epochs of *VI* data. We found and determined periods for more than 500 RR Lyrae, 17 anomalous Cepheids, 6 Population II Cepheids. In addition we have 85 candidate Long Period Variables, the majority of which were previously unknown. We estimated that the average metal abundance of RR Lyrae stars is $[\text{Fe}/\text{H}] \simeq -1.6$ dex.

Subject headings: galaxies: individual: Fornax — stars: RR Lyrae — distance scale — stars: variable

1. Introduction

Several studies have found variable stars in Fornax or have detected variability (Light et al. 1986, Demers & Irwin 1987, Buonanno et al. 1985, Stetson et al. 1998). However they all suffered from some limitations. For instance Stetson et al. (1998) cover a large area with deep photometry but they don't have enough epochs to determine periods for their candidate variables. Light et al. (1986) did have a lot of data but they covered a very small area; they have light curves for only two variable stars. Demers & Irwin (1987) covered the whole galaxy and had ~ 20 epochs but their photometry didn't go deep enough to detect RR Lyrae. For these reasons, there are few variable stars known in Fornax with published periods and light curves. We thus thought that it would be worthwhile to survey a fair fraction of this galaxy and look for variable stars, in particular RR Lyrae stars.

2. Observations, data reduction and photometry

Imaging observations of Fornax were made with the 1m telescope at Siding Spring Observatory and with the 1.3m telescope at Mount Stromlo Observatory. Roughly half the epochs of observation came from each telescope. Table 1 lists the dates of observation for each field. The two sets of observations are described separately below.

2.1. Observations at Siding Spring Observatory

The part of the data obtained with the 1m telescope at Siding Spring Observatory was taken during two runs of a few consecutive nights. We used a SITe 2048×2048 CCD that gives a field of view of $20.5' \times 20.5'$ (0.602 arcsecond per pixel). Four fields have been observed in V and I_C filters, covering a square on the sky. The four fields were centered approximately on $\alpha_1 = 2^h 40^m 26.0^s$, $\delta_1 = -34^\circ 28' 40''$, $\alpha_2 = 2^h 38^m 40.0^s$, $\delta_2 = -34^\circ 28' 40''$, $\alpha_3 = 2^h 40^m 26.0^s$, $\delta_3 = -34^\circ 50' 00''$, $\alpha_4 = 2^h 38^m 40.0^s$, $\delta_4 = -34^\circ 50' 00''$ (thus field 1 is north-east, field 2 is north-west, field 3 is south-east and field 4 is south-west). The total area observed is almost half a square degree, covering the central regions of the galaxy. Each field has been observed between one and four times per night, with a typical exposure time of 10 minutes, resulting in about 12 to 15 exposures per field. Our average seeing is $2''$, with the best value being $1.5''$. During two nights we also observed standard stars taken from the list of Landolt (1992).

The data have been processed in a standard way using IRAF¹ procedures. We performed aperture photometry for the standard stars and solved the transformation equations between the instrumental and standard systems. We obtained

$$m_{std,V} = m_{obs,V} + const_V - 0.161X - 0.065(V - I), \quad (1)$$

$$m_{std,I} = m_{obs,I} + const_I - 0.071X - 0.039(V - I) \quad (2)$$

where m_{std} is the magnitude of the standard star, m_{obs} is the actually observed magnitude, X is the airmass and $(V - I)$ is the color of the star. The residuals were 0.010 *mag* in V and 0.011 *mag* in I . The extinction coefficients are close to the average values found for SSO (Sung & Bessell 2000) and the color terms are virtually identical to those found by Sung et al. (1998) for the particular camera and filter set that we used.

The photometry for each Fornax frame was extracted using DoPHOT (Schechter et al. 1993) in fixed position mode. We first created a “template” frame for each field. Each template is the average of 4-6 good seeing images. Photometry was done on this deep template and the star list of the template was used as input for the photometry of each program frame. Then all images were put on the same zero-point (still in the instrumental system). We applied an aperture correction to these magnitudes and Eqs (1) and (2) were inverted to provide calibrated photometry for each frame. We estimate that our absolute zero point is accurate to ~ 0.02 *mag*.

2.2. Observations at Mount Stromlo Observatory

We obtained 20 images with the wide-field camera mounted on the Mount Stromlo Observatory 50" telescope (MSO). This camera was used by the MACHO project and is a mosaic of four $2k \times 2k$ CCD with a pixel scale of $0.628''/\text{pixel}$, covering approximately $42' \times 42'$. A feature of this camera is a dichroic mirror that allows to obtain simultaneous measurements in two passbands, V_M and R_M , corresponding (very roughly) to V and R . We refer the reader to Stubbs et al. (1993) and Alcock et al. (1999) for descriptions of the camera system and filters. The exposure time was 10 minutes for each image. The typical seeing was $2.2''$.

Photometry was also performed in fixed-position mode and the frames were then put on a common zero point. Since the passbands are non-standard, we needed to calibrate V_M and R_M to V and I . For this we

¹IRAF is distributed by the National Optical Astronomy Observatories, which are operated by the Association of Universities for Research in Astronomy, Inc., under cooperative agreement with the National Science Foundation.

could use our already calibrated photometry from the 1m SSO telescope. The passbands V_M and R_M are quite broad but they have been calibrated to V and R (Bessell & Germany 1999, Alcock et al. 1999).

The areas covered with each telescope/instrument combination are virtually identical, thus we have VI and $V_M R_M$ photometry for most stars. Figure 1 illustrates the procedure we used to calibrate the color $V_M - R_M$ to $V - I$. For each chip, we constructed plots like Fig. 1 and plots of $I - R_M$ vs $V_M - R_M$. The “knee” at $V_M - R_M \simeq 1.3$ can already be found in Bessell & Germany (1999) in a $V - R_M$ vs $V_M - R_M$ diagram (their Fig. 5). This knee also happens when we use $V - I$ since there is an almost linear relation between $V - I$ and $V - R$. We then made separate fits for stars bluer and redder than $V_M - R_M = 1.3$. For blue stars ($V_M - R_M \leq 1.3$) a typical calibration would be

$$V - I = 1.123(V_M - R_M) + 0.069 \quad (3)$$

$$I - R_M = -0.341(V_M - R_M) - 0.141 \quad (4)$$

and for red stars ($V_M - R_M > 1.3$)

$$V - I = 2.024(V_M - R_M) - 1.083 \quad (5)$$

$$I - R_M = -0.842(V_M - R_M) + 0.502 \quad (6)$$

From chip to chip there were slight differences in the coefficients, amounting to a few percents at most. Our separate chip-by-chip calibration might not have been warranted (the approach followed by Bessell & Germany 1999). However, we certainly do not lose accuracy in the process, it is only a little more cumbersome.

After the calibration of the whole data set an astrometric calibration was done, using the USNO-A2.0 catalog (Monet et al. 1998) giving residuals between 0.3 and 0.5 arcseconds.

With calibrated photometry in hand, the last step is to apply a reddening correction. Given the high Galactic latitude of Fornax ($b \sim -66^\circ$), the average reddening should be very low. We thus used the maps of Schlegel et al. (1998) to determine the reddening to every star in our data set. The average $E(B - V)$ is around 0.025 mag.

3. Search for variables

We used the method proposed by Welch & Stetson (1993). It makes use of the fact that when a star is brighter (or fainter) than average in one passband it is also brighter (fainter) than average in another passband. The variability index I_{WS} has been computed for each star, and Fig 2 presents the results. Fig 3 shows the color-magnitude diagram with the variables we have identified.

Fornax has five globular clusters (Hodge 1961), two of which are in our field (cluster 2 and cluster 4). However it was impossible to find variables in these clusters, because of the exceedingly high density of stars. While it is possible to resolve some stars in cluster 2 (no star could be resolved in cluster 4), the effect of a varying seeing made the photometry extremely unreliable, although we found one candidate Long Period Variable in cluster 2. Detection of RR Lyrae in Fornax’s globular clusters can only be done with a much better spatial resolution than we have.

The probability of detecting a variable star depends on a number of things, an important one being the actual time distribution of the observations, since this can affect the detection of some periods more than others. We carried out numerical simulations (much in the spirit of Saha & Hoessel, 1990) to estimate the impact that our sampling may have on the discovery of variable stars. For a star of period P and initial phase ϕ_0 (phase at the time of the first observation), we can compute the phase at each of our observations. We then determine which of the following criteria are fulfilled:

1. At least 3 observations between phases 0 and 0.2 ($\phi = 0$ corresponds to maximum light)
2. At least 2 phases between 0.2 and 0.5 (descending light)
3. At least 3 phases between 0.5 and 0.8 (around minimum light)
4. At least 15 measurements in total

For all periods between 0.1 and 50 days, and for all initial phases, we simply count the number of observations satisfying each criterion, after having attributed a weight to each observation: we estimate that the *photometric* detection efficiency of the SSO 40" data is 0.8, and 0.4 for the MSO 50" data. This means that, for instance, four actual SSO 40" observations are needed to satisfy criterion 1. For each period we then count the number of phases that fulfill these criteria. After appropriate normalization, we obtain a period spectrum which is simply the probability of detecting a star as a function of period (see Fig 4).

3.1. RR Lyrae stars

We selected all stars in a broad region around the horizontal branch in order to look for RR Lyrae variables. Specifically the criteria were $20.8 \leq V \leq 21.6$, $0.2 \leq V - I \leq 0.8$ and $I_{WS} > 0.9$. Our data are somewhat inhomogeneous in the sense that that SSO 40" data are of better quality than the MSO 50" data. In the search for RR Lyrae we thus used only SSO data when computing the I_{WS} index. The value $I_{WS} = 0.9$ has been chosen as a compromise between finding the largest number of genuine variables while minimizing the number of false detections. It can be seen from Fig 2 that the bulk of the stars are below $I_{WS} = 0.9$. Applying the criteria given above yielded 851 objects.

We used the phase-dispersion minimization algorithm (Stellingwerf, 1978) to look for periodicity in V -band data. A rapid inspection of some light curves revealed that for a fairly large number of candidates no period could give a reasonable light curve. This is because the magnitude of a RR Lyrae variable is close to the detection limit of our photometry. We thus decided to apply a conservative approach and to select the best period by examining each light curve. This led to rejecting a fairly large number of candidates. Our goal was to produce a reasonably clean sample of RR Lyrae, not a complete one. Among the stars rejected, a significant number may be genuine RR Lyrae.

The main reason to reject a candidate variable was the total number of measurements per star. Among the rejected candidates, 48% had less than 25 measurements whereas 75% of the confirmed RR Lyrae have more than 25 data points. There is no obvious correlation between the value of the variability index I_{WS} and the probability of finding a period. This is because we used ~ 15 epochs to construct the index I_{WS} (only SSO 40" data). Some stars may show a large I_{WS} but may have only 15 measurements, making it difficult to find a reliable period. The second reason for rejecting a variable is aliasing. For some stars it was impossible to decide between two periods. In particular, for a given frequency ν , the light curves for $1 - \nu$ or

$1 + \nu$ would be almost as convincing as ν . In the end, this selection yielded 515 RR Lyrae stars for which one single frequency could be clearly identified, hence 60% of our candidates turned out to be “good” RR Lyrae variables. They are listed in Table 2 where we give the phase-weighted average magnitudes and associated uncertainties. Some light curves are shown in Fig. 5. When considering the I -band light curves in this figure, it is quite remarkable that the Welch-Stetson method still works, even though the variability signal is extremely weak in the I band. This shows that the method is very powerful even at faint magnitudes. One has to bear in mind that the number of variables is likely to be a lower limit to the total number of RR Lyrae stars in Fornax. In particular, a consequence of the quality of our data (the average measurement error for a typical RR Lyrae variable is ~ 0.15 mag) is that our survey is probably biased against RRc variables, which have a low amplitude. This will affect the relative number of RRab and RRc variables but the incompleteness should not depend on period. With better photometric data it will be possible to obtain good light curves for many more RR Lyrae.

The period histogram is shown on Fig. 6. There are two peaks, one at ~ 0.57 days and one at ~ 0.38 days. There seems to be a gap between 0.46^d and 0.48^d . The probability of detecting variables with periods around 0.5^d is very low but for periods $0.46^d \leq P \leq 0.48^d$ our detection probability is always larger than 66% of the maximum (see Fig. 6) so we should be able to discover variables with periods between 0.46^d and 0.48^d , if they exist. We thus interpret this gap as the transition period from RRab to RRc. The shortest period for RRab type is thus 0.48^d . Given that our data are not good enough to determine the type of variable on the basis of the light curve, we *defined* RRab type variables as the stars having periods larger than 0.47 days, and RRc as having periods shorter than 0.47 days. The number of stars in each category is $N_{ab} = 396$ and $N_c = 119$. We then determined the average periods $\langle P_{ab} \rangle = 0.585^d$ and $\langle P_c \rangle = 0.349^d$. The longest period for RRab variables is 0.737^d .

In galactic globular clusters, the average period of ab type RR Lyrae variables $\langle P_{ab} \rangle$ is either near 0.55^d or near 0.64^d (Oosterhoff class I and II respectively). The surprising fact is that dwarf spheroidal galaxies do not fall in either of these categories. From Table 7 in Mateo et al. (1995), one sees that all dwarf spheroidal galaxies are intermediate between Oo I and Oo II categories. Adding the result of Siegel & Majewski (2000) for Leo II ($\langle P_{ab} \rangle = 0.619^d$) and the present value of 0.585^d for Fornax only reinforces this statement.

The average properties of RR Lyrae variables are related to their metallicity. There are relations between several characteristic periods (longest, shortest, average) and the metal content (Sandage 1993). For the shortest period one has

$$\log P_{ab} = -0.122(\text{[Fe/H]}) - 0.500 \quad (7)$$

which yields $[\text{Fe/H}] = -1.5$ (for $P_{ab} = 0.48^d$). Through the relation

$$\log \langle P_{ab} \rangle = -0.092(\text{[Fe/H]}) - 0.389 \quad (8)$$

the average period yields $[\text{Fe/H}] = -1.7$. The longest period is related to $[\text{Fe/H}]$ via

$$\log P_{ab} = -0.09(\text{[Fe/H]}) - 0.280 \quad (9)$$

which gives $[\text{Fe/H}] = -1.64$. All these values of $[\text{Fe/H}]$ are on the Butler-Blanco metallicity scale (used by Sandage) which is more metal-rich than the widely used scale of Zinn & West (1984) by 0.2 dex.

When considering in particular the average period $\langle P_{ab} \rangle$, there is some scatter in this relation, about 0.2 dex (see Siegel & Majewski 2000, their figure 6, which also displays the other eight dwarf spheroidal

galaxies). Our estimates of the metal abundance cluster around ≈ -1.6 , we will then take as a final value $[\text{Fe}/\text{H}] = -1.6 \pm 0.2$.

In contrast with this small dispersion in $[\text{Fe}/\text{H}]$ is the fairly large dispersion in average magnitudes for RR Lyrae stars ($\sigma = 0.140$). This is significantly larger than what is observed in other dwarf spheroidal galaxies [e.g. $\sigma = 0.096$ in Leo II – Siegel & Majewski (2000), $\sigma = 0.104$ in Sculptor – Kaluzny et al. (1995)]. It seems likely that photometric scatter is responsible for the dispersion in $\langle V \rangle$.

3.2. Population II and anomalous Cepheids

We found a number of variables slightly or significantly brighter than the horizontal branch, most of which are anomalous Cepheids (ACs) or Population II Cepheids. Their magnitudes and periods are given in Table 3. We found 6 Pop II Cepheids (one unsure), 17 anomalous Cepheids (one unsure) and one blue variable whose nature is unclear.

The position of a variable in the period-luminosity diagram (Fig. 8) is determined by its metallicity and pulsation mode (e.g. Nemec et al 1994). Fornax has a large range in $[\text{Fe}/\text{H}]$ and it has had a complex star formation history (Saviane et al. 2000). This means that Cepheids in this galaxy can have a range of ages and/or metallicities. Unfortunately, in the absence of any information on $[\text{Fe}/\text{H}]$ it is impossible to assign a pulsation mode to these variables. By looking at Fig 8 it is clear however that there must be a range of metallicity among these stars. Some of the extreme stars in Fig. 8 could be metal-poor and overtone pulsators while others are metal-rich and fundamental pulsators.

There is a surprising correlation between the specific frequency of anomalous Cepheids and the luminosity of the dwarf spheroidal galaxies (Mateo et al. 1995). According to this relation, about a dozen anomalous Cepheids should have been found. We found 17, fairly close to the prediction and not large (nor small) enough to destroy the correlation found by Mateo et al. (1995). The nature of anomalous Cepheids is unclear. They are found in systems where the most massive stars still burning nuclear fuel are $\approx 0.8M_{\odot}$, however the masses of anomalous Cepheids are around $\sim 1.5M_{\odot}$ (e.g. Wallerstein & Cox 1984, Bono et al. 1997) The two explanations usually put forward to explain their large masses are that they are intermediate-age stars or that they are the product of a binary star merging (the two component having the mass of a turn-off star). Fornax has an important intermediate-age population so the first hypothesis is perfectly plausible, however it is not easy to rule out the second possibility.

A remarkable fact is that, among the nine dwarf galaxies satellites of the Milky Way, Fornax is the only one containing Pop. II Cepheids. These stars are in a short-lived evolutionary stage and Fornax is probably the only dwarf galaxy that is massive enough to have a few of these stars.

3.3. Long Period Variables

There has already been a wide-field survey for Long Period Variables (LPVs) in Fornax (Demers & Irwin 1987). They covered the whole galaxy and found 30 variables. It was based on photographic plates obtained at the UK Schmidt telescope and they acknowledge the fact that “a certain number of bright variables must have been missed ... because of blended images”. It thus seemed worthwhile to look specifically for bright red variables showing a long-term trend, even though our sampling is far from ideal for these stars. Demers & Kunkel (1979) presented a list of very red stars in Fornax. Based on two V measurements separated by

132 days, they could flag some of these stars as candidate variables. We also tried to recover objects from that paper.

Eighty five stars turn out to be reasonably good candidates. They are given in Table 4. In this table, a question mark means that the variability is not certain; this happens particularly for crowded stars. Given that our data do not allow to obtain periods for such objects, the classification as LPVs is only tentative. However, given their magnitudes and colors, most objects in Table 4 are good candidates. In this Table we also indicate the numbers given by Stetson et al. (1998) in their Table 1 for red stars.

We have data for 19 variables listed by Demers & Irwin (1987), 3 of which appear non variable in our data simply because we don't have enough measurements. The remaining 11 stars in the list of Demers & Irwin are not in our survey area. In addition we find 38 good candidate LPVs and 28 possible variables (indicated with a ? in Table 4). In Fig. 9 we show two examples of LPVs.

There are a few dozens of red giants ($V < 19$, $V - I > 1$) showing some variability (i.e. with $I_{WS} > 0.9$), most with small amplitude (less than 0.1 *mag*). Variability along the red giant branch has been detected in a number of cases in Galactic field and globular clusters giants (e.g. Smith & Dupree 1988 and references therein), however it is not clear whether this is related to pulsation, spots, or any other mechanism. The typical periods of these objects are likely to be in the range of days to weeks, where our ability to find a period is seriously affected by the sampling (see Fig 4).

4. Discussion

We have presented a survey of 1/2 square degree covering the central region of the Fornax dwarf galaxy. We found and determined periods for 17 anomalous Cepheids, 6 Population II Cepheids and more than 500 RR Lyrae. In addition, 85 LPV candidates were identified. It is almost certain that there are more RR Lyrae in this galaxy: the accuracy of our data do not allow us to produce a complete catalog of RR Lyrae. The average metal abundance of RR Lyrae is $[\text{Fe}/\text{H}]_{RR} \simeq -1.6 \pm 0.2$.

We can use the known distance to Fornax ($\mu_0 = 20.68$ with the tip of the red giant branch, Bersier 2000) to estimate the brightness of RR Lyrae. With an average magnitude of $\langle V_0 \rangle = 21.27$, one obtains $M_V(RR) = 0.59 \pm 0.1$ *mag*. This is intermediate between other estimates of the magnitude of RR Lyrae stars. Gould & Popowski (1998) found $M_V(RR) \simeq 0.75$ for $[\text{Fe}/\text{H}] = -1.7$, while from Sandage (1993) one would get $M_V = 0.40$ *mag*.

We thank the director of Mt Stromlo & Siding Spring Observatories, Jeremy Mould, for the allocation of director's discretionary time on the MSO 50" telescope. We also thank the referee for a swift and constructive report that helped us improve this paper. DB acknowledges partial support from the Swiss National Science Foundation (grant 8220-050332). This work has also been supported by NSF grant AST-9979812.

REFERENCES

Alcock, C. et al. (The MACHO collaboration) 1999, PASP, 111, 1539
Bersier, D. 2000, ApJ, 543, L23
Bessell, M. S., Germany, L. M. 1999, PASP, 111, 1421

Demers, S., Irwin, M. J. 1987, MNRAS, 226, 943

Demers, S., Kunkel, W.E. 1979, PASP, 91, 761

Gould, A., Popowski, P., 1998, ApJ, 508, 844

Hodge, P. W 1961, AJ, 66, 83

Kaluzny, J., Kubiak, M., Szymański, M., Udalski, A., Krzeminski, W., Mateo, M 1995, A&AS, 112, 407

Landolt, A. U., 1992, AJ, 104, 340

Light, R. M., Armandroff, T. A., Zinn, R. 1986, AJ, 92, 43

Mateo, M., Fischer, P., Krzeminski, W. 1995, AJ, 110, 2166

Monet, D., et al. 1998, USNO-SA2.0, (Washington: US Naval Obs.)

Nemec, J. M., Nemec, A. F. L., Lutz, T. E. 1994, AJ108, 222

Saha, A., Hoessel, J.G. 1990, AJ, 99, 97

Sandage, A. 1993, AJ, 106, 687

Sandage, A. 1993, AJ, 106, 703

Saviane, I., Held, E. V., Bertelli, G. 2000, A&A355, 56

Schechter, P. L., Mateo, M., Saha, A., 1993, PASP, 105, 1342

Schlegel, D. J., Finkbeiner, D. P., Davis, M. 1998, ApJ, 500, 252

Siegel, M. H., Majewski, S. R. 2000, AJ, 120, 284

Smith, G. H., Dupree, A. K., 1988, AJ, 95, 1547

Stellingwerf, R. F. 1978, ApJ, 224, 953

Stetson, P. B., Hesser, J. E., Smecker-Hane, T. A. 1998, PASP, 110, 533

Stubbs, C., et al. (The MACHO collaboration) 1993, Proc. SPIE, 1900, 192

Sung, H., Bessell, M. S., Lee, S.-W. 1998, AJ, 115, 734

Sung, H., Bessell, M. S. 2000, PASA, 17, 244

Udalski, A., Kubiak, M., Szymanski, M., Kaluzny, J., Mateo, M., Krzeminski, W., 1994, AcA, v.44, 317

Walker, A.R. 1994, AJ, 108, 555

Wallerstein, G., Cox, A.N. 1984, PASP, 96, 677

Welch, D. L., Stetson, P.B. 1993, AJ, 105, 1813

Zinn, R., West, M. J. 1984, ApJS, 55, 45

Table 1: Journal of observations.

Field	JD _V	JD _I	Observatory
1	652.26667	652.26667	MSO
1	657.26976	657.26976	MSO
1	658.27549	658.27549	MSO
1	659.28311	659.28311	MSO
1	660.25075	660.25075	MSO
1	661.23904	661.23904	MSO
1	662.23573	662.23573	MSO
1	663.23345	663.23345	MSO
1	664.23512	664.23512	MSO

Note. — Table 1 is presented in its complete form in the electronic version of the journal. Only a fraction is shown here for guidance regarding its form and content.

Table 2: RR Lyrae variables.

Name	<i>N_V</i>	<i>V</i>	σ_V	<i>N_I</i>	<i>I</i>	σ_I	<i>I_{WS}</i>	Period (days)	<i>E(B – V)</i>
FBW J023749.8-342427	24	21.389	0.027	24	20.755	0.036	1.422	0.54365	0.028
FBW J023750.8-342736	32	21.346	0.021	31	20.744	0.035	2.741	0.58252	0.030
FBW J023751.9-342620	32	21.419	0.023	32	20.887	0.033	1.139	0.58052	0.029
FBW J023752.8-344615	32	21.469	0.029	32	20.560	0.033	2.005	0.16459	0.034
FBW J023753.4-345215	28	21.344	0.026	28	20.781	0.035	1.584	0.59260	0.035
FBW J023755.0-343726	30	21.401	0.026	29	20.911	0.035	1.506	0.40322	0.035
FBW J023756.0-342732	32	21.468	0.020	32	21.101	0.036	5.965	0.33797	0.030
FBW J023756.1-344332	31	21.544	0.022	31	20.849	0.036	2.666	0.51202	0.034
FBW J023756.6-343507	32	21.392	0.022	32	20.766	0.031	2.208	0.54362	0.035
FBW J023757.0-342201	32	21.455	0.021	32	20.838	0.032	2.497	0.56046	0.028

Note. — Table 2 is presented in its complete form in the electronic version of the journal. Only a fraction is shown here for guidance regarding its form and content.

Table 3: Anomalous Cepheids and Population II Cepheids

Name	V	$V - I$	σ_V	σ_I	$E(B - V)$	Period	Class
FBW J023803.9-343822	19.478	0.483	0.007	0.012	0.036	15.2283	P2C
FBW J023811.9-344023	20.651	1.087	0.015	0.021	0.036	1.21327	P2C
FBW J023843.0-344825	19.801	0.558	0.016	0.031	0.031	1.04503	AC
FBW J023852.4-343012	19.905	0.602	0.007	0.011	0.027	1.24968	AC
FBW J023853.4-343048	19.712	0.564	0.006	0.010	0.027	2.57976	P2C
FBW J023907.1-343316	20.786	0.774	0.017	0.025	0.026	0.50812	AC
FBW J023926.9-342806	20.272	0.667	0.010	0.016	0.025	2.08323	P2C
FBW J023926.8-343122	20.828	0.673	0.017	0.028	0.024	0.50398	AC
FBW J023927.0-342427	21.052	0.082	0.019	0.042	0.026	0.56965	blue
FBW J023937.7-343621	20.645	0.725	0.015	0.024	0.025	0.546	AC
FBW J023941.5-343125	20.616	0.475	0.012	0.022	0.024	0.57345	AC
FBW J023945.2-344314	21.230	0.481	0.019	0.037	0.024	1.14259	P2C?
FBW J023946.2-343001	20.568	0.786	0.014	0.023	0.023	0.92161	AC
FBW J023952.5-343340	20.252	0.904	0.014	0.023	0.024	1.31071	AC
FBW J023953.5-342433	20.846	0.656	0.015	0.026	0.022	0.61144	AC
FBW J023954.8-343601	21.022	0.478	0.016	0.031	0.025	0.57442	AC
FBW J024000.9-341846	20.828	0.476	0.015	0.025	0.023	0.41592	AC
FBW J024002.7-341928	20.362	0.849	0.009	0.015	0.022	0.53299	AC
FBW J024010.2-343212	20.624	0.412	0.013	0.025	0.022	1.33531	P2C
FBW J024016.9-343641	20.840	0.430	0.014	0.030	0.025	0.53294	AC
FBW J024017.4-342024	19.994	0.608	0.007	0.011	0.021	1.19847	AC
FBW J024022.8-342802	20.480	0.526	0.011	0.019	0.020	0.83757	AC
FBW J024050.2-344335	20.826	0.729	0.015	0.024	0.024	0.50578	AC
FBW J024058.3-344552	20.786	0.663	0.018	0.028	0.024	0.48106	AC

Table 4: Candidate and known Long Period Variables.

Name	N_V	V^a	σ_V^b	N_I	$V - I^a$	σ_{V-I}^b	$E(B - V)$	Other ID ^c	Note ^d
FBWJ023800.0-344422	32	18.562	0.021	32	1.860	0.026	0.034		
FBWJ023806.1-343119	30	20.233	0.065	30	3.765	0.070	0.033		
FBWJ023812.6-345606	32	18.504	0.022	32	2.291	0.026	0.033	DK1, DI30	
FBWJ023817.1-342548	32	18.591	0.023	32	2.314	0.030	0.029	S3, DI13	
FBWJ023821.3-343618	32	18.335	0.021	32	1.942	0.026	0.034		?
FBWJ023822.0-345213	32	17.960	0.014	32	1.577	0.019	0.032		
FBWJ023822.6-343804	32	18.731	0.023	31	2.296	0.029	0.035	DK15	
FBWJ023826.3-342533	30	18.451	0.017	30	1.649	0.022	0.029		
FBWJ023830.2-344503	28	18.324	0.017	28	1.875	0.021	0.033		
FBWJ023833.4-342824	32	18.403	0.018	32	1.717	0.025	0.029		?

^aThe magnitudes are arithmetic averages.

^bThe σ s are the average measurement errors.

^cNumber preceded by S are from Table 1 of Stetson et al. (1998), numbers preceded by DK are from Demers & Kunkel (1979), numbers preceded by DI are from Demers & Irwin (1987).

^dA ? means that the variability is not certain.

Note. — Table 4 is presented in its complete form in the electronic version of the journal. Only a fraction is shown here for guidance regarding its form and content.

Fig. 1.— The color ($V - I$) as a function of MACHO color ($V_M - R_M$). The two segments of straight lines show the calibration applied to the data

Fig. 2.— The variability index I_{WS} as a function of magnitude. Stars with $I_{WS} \geq 0.9$ have a large probability of being variable. The vertical “finger” at $m_V \simeq 21.3$ is caused by RR Lyrae.

Fig. 3.— The color-magnitude diagram. Note that the magnitudes of non-variable stars are the average of 12 measurements. Crosses are for RR Lyrae, triangles are for anomalous and Population II Cepheids, hexagons are for Long Period Variables.

Fig. 4.— The probability of detecting variable stars as a function of period for field 1 (see text for explanations). *Upper panel*: for periods between 0.1^d and 50^d , *Lower panel*: for periods between 0.1^d and 1^d .

Fig. 5.— V and I light curves of six RR Lyrae variables, including the longest period one (bottom right). The period is indicated for each star in the upper left part of the V panel.

Fig. 6.— (*Solid line*) The period histogram for all confirmed RR Lyrae. The absence of variables with periods near 0.46 days suggest that this is the transition period between RRab and RRc type variables. (*Dashed line*) The detection probability for field 2

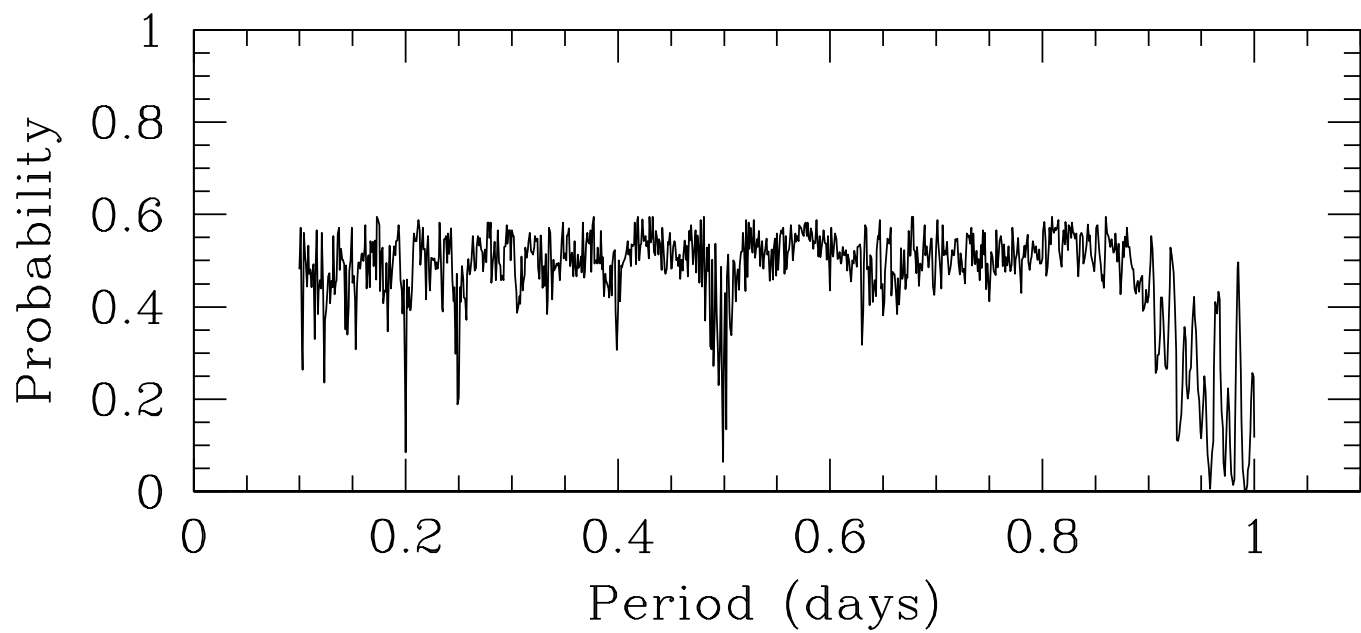
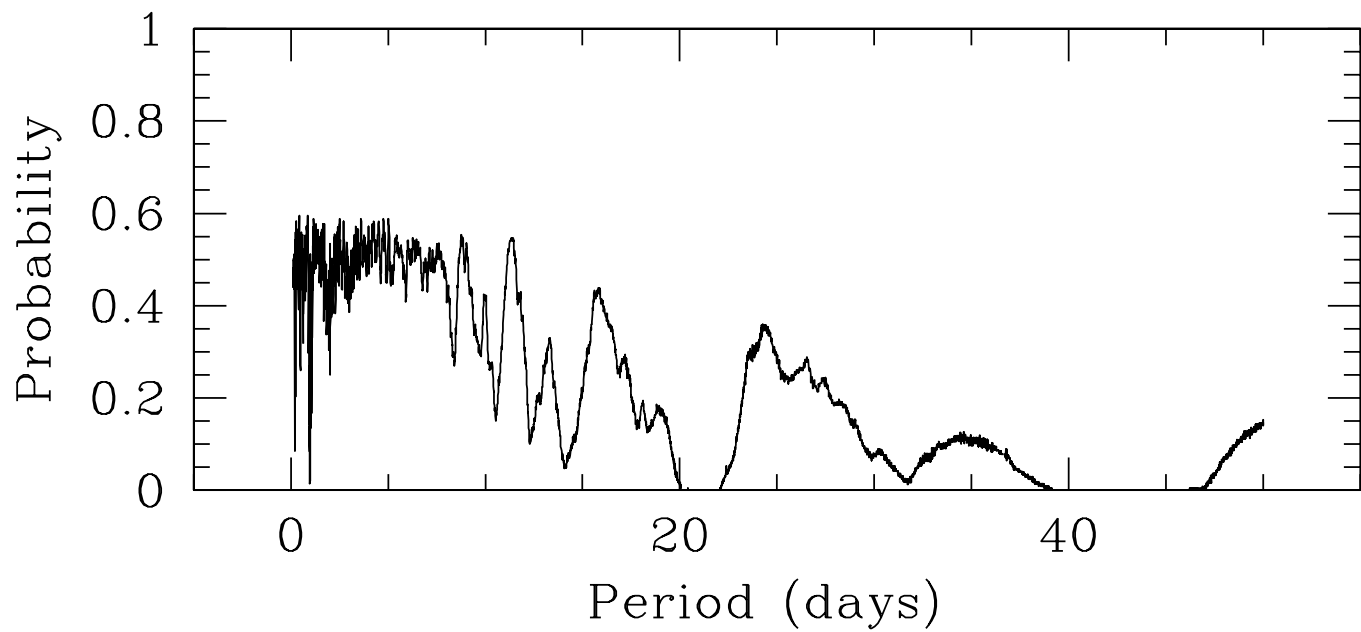
Fig. 7.— The top panels show the V and I light curves of two anomalous Cepheids; the bottom panels show the light curves of two Pop II Cepheids. The periods are indicated in each case.

Fig. 8.— The period-luminosity plot for anomalous Cepheids (squares) and Population II Cepheids (stars). The solid lines are the PL relations for fundamental and first overtone modes from Nemec et al. (1994) with $[\text{Fe}/\text{H}] = -2$, shifted to correspond to a distance modulus of 20.66 mag (Bersier 2000); the dotted lines are the same for $[\text{Fe}/\text{H}] = -1$. The cross indicates the average position of RR Lyrae stars.

Fig. 9.— V and I data for two candidate Long Period Variables. The top one is DI13, the second has not been found by Demers & Irwin (1987). The triangles are for I -band data, squares are for V -band data.

This figure "cmdvar.jpg" is available in "jpg" format from:

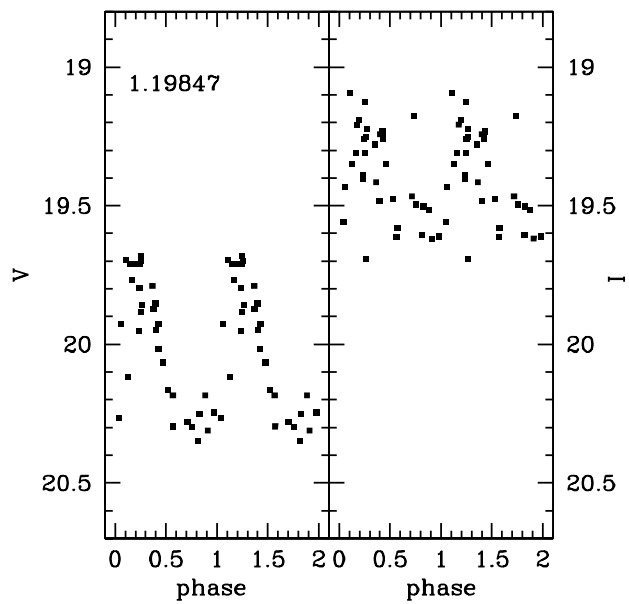
<http://arxiv.org/ps/astro-ph/0110555v1>



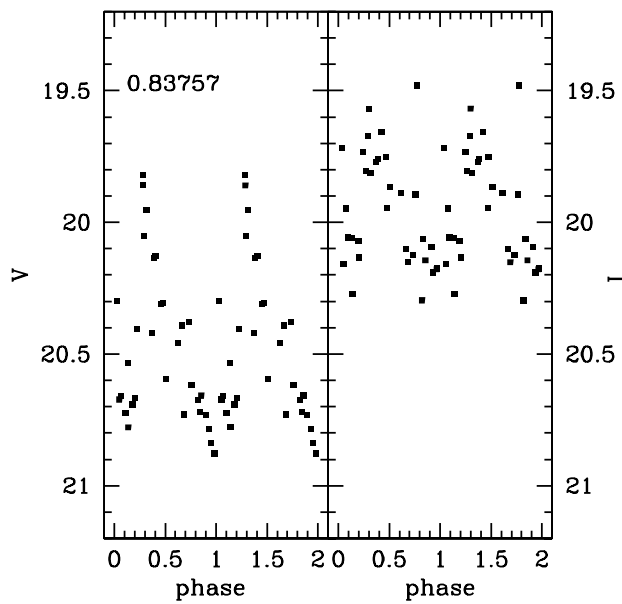
This figure "iws.jpg" is available in "jpg" format from:

<http://arxiv.org/ps/astro-ph/0110555v1>

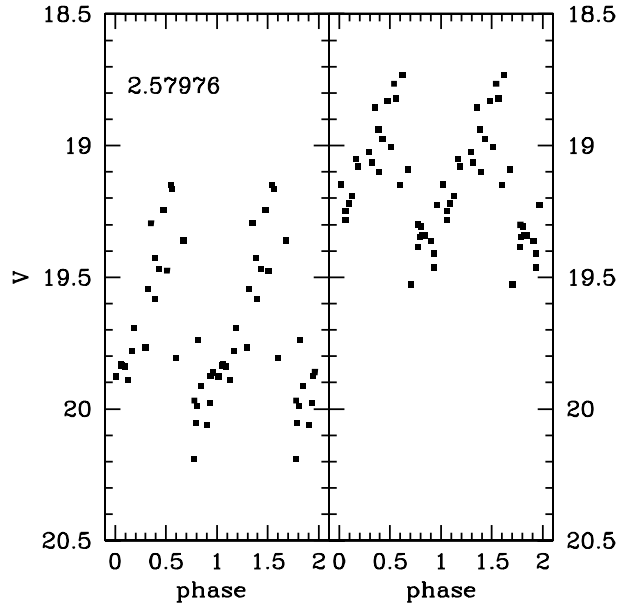
FBW J024017.4-342024



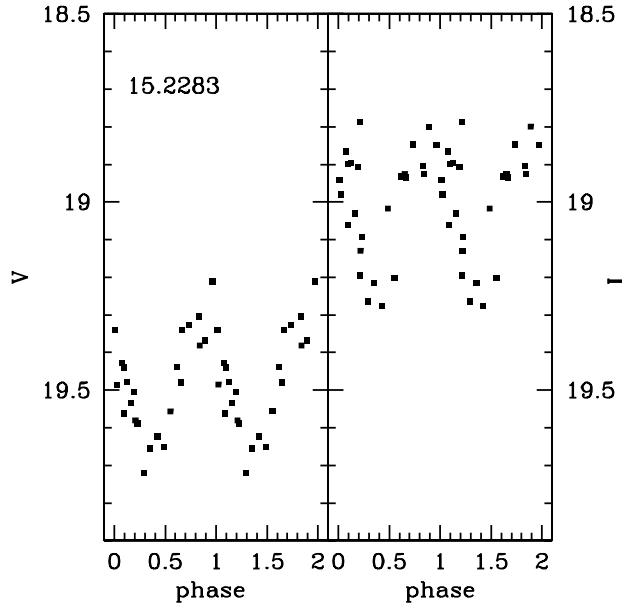
FBW J024022.8-342802



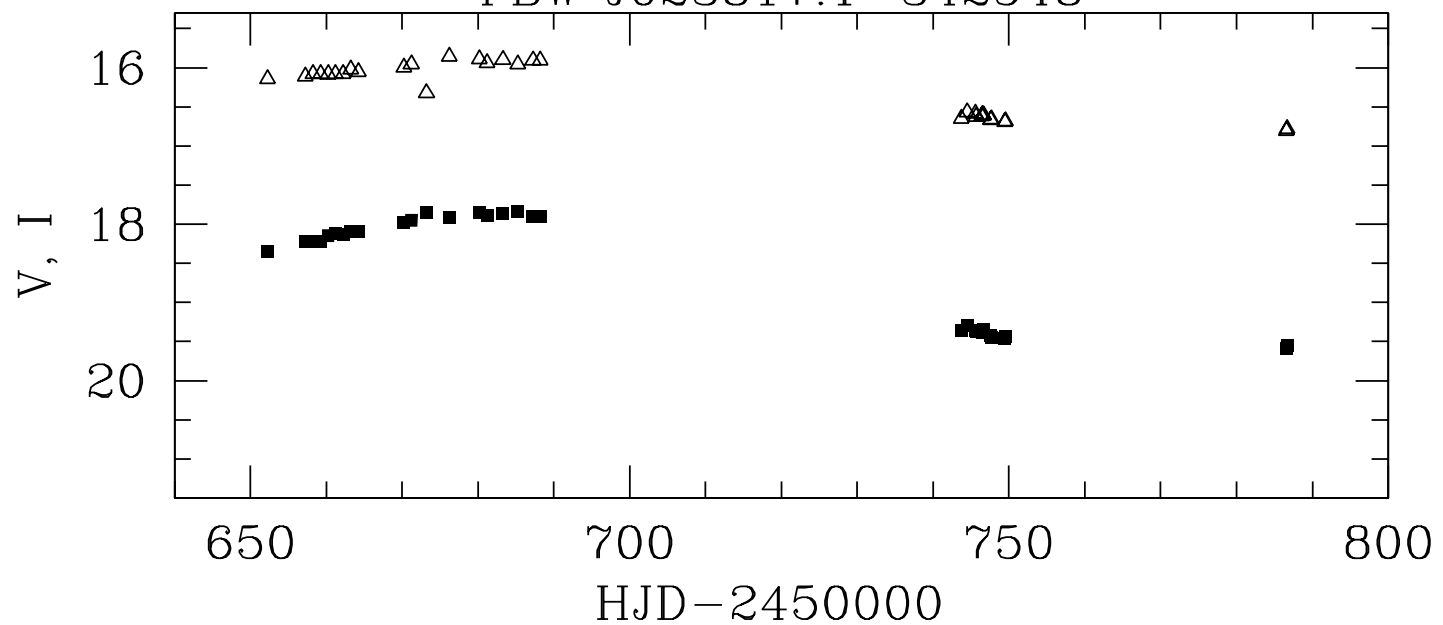
FBW J023853.4-343048



FBW J023803.9-343822



FBW J023817.1-342548



FBW J023853.0-344919

